International Journal of Medical Microbiology 305 (2015) 157–169

Contents lists available at ScienceDirect

International Journal of Medical Microbiology

journal homepage: www.elsevier.com/locate/ijmm

Stress-triggered signaling affecting survival or suicide of *Streptococcus pneumoniae*

Paulo R. Cortes [1], Germán E. Piñas [1,2], Melina B. Cian [1], Nubia Yandar, Jose Echenique *

Departamento de Bioquímica Clínica-CIBICI (CONICET), Facultad de Ciencias Químicas, Universidad Nacional de Cordoba, Medina Allende esq. Haya de la Torre, Ciudad Universitaria, CP, X5000HUA Cordoba, Argentina

ARTICLE INFO

Article history:
Received 12 June 2014
Received in revised form 1 December 2014
Accepted 1 December 2014

Keywords:
Streptococcus pneumoniae
F_0F_1-ATPase
Two-component systems
Acidic stress
Autolysis
ATR
LytA
Intracellular

ABSTRACT

Streptococcus pneumoniae is a major human pathogen that can survive to stress conditions, such as the acidic environment of inflammatory foci, and tolerates lethal pH through a mechanism known as the acid tolerance response. We previously described that *S. pneumoniae* activates acidic-stress induced lysis in response to acidified environments, favoring the release of cell wall compounds, DNA and virulence factors.

Here, we demonstrate that F_0F_1-ATPase is involved in the response to acidic stress. Chemical inhibitors (DCCD, optochin) of this proton pump repressed the ATR induction, but caused an increased ASIL. Confirming these findings, mutants of the subunit *c* of this enzyme showed the same phenotypes as inhibitors. Importantly, we demonstrated that F_0F_1-ATPase and ATR are necessary for the intracellular survival of the pneumococcus in macrophages.

Alternatively, a screening of two-component system (TCS) mutants showed that ATR and survival in pneumocytes were controlled in contrasting ways by ComDE and CiaRH, which had been involved in the ASIL mechanism. Briefly, CiaRH was essential for ATR (ComE represses activation) whereas ComE was necessary for ASIL (CiaRH protects against induction). They did not regulate F_0F_1-ATPase expression, but control LytA expression on the pneumococcal surface.

These results suggest that both TCSs and F_0F_1-ATPase control a stress response and decide between a survival or a suicide mechanism by independent pathways, either in vitro or in pneumocyte cultures. This biological model contributes to the current knowledge about bacterial response under stress conditions in host tissues, where pathogens need to survive in order to establish infections.

Introduction

Streptococcus pneumoniae (or the pneumococcus) is one of the main human pathogens, being the causal agent of otitis and sinusitis, as well as of more severe diseases such as pneumonia, bacteremia and meningitis. During the infection process, *S. pneumoniae* has to be able to survive the environmental stress found in different host tissues. Related to this, it has been described that an acidic environment (pH 5.5–7.0) is a common characteristic of the acute inflammation produced by bacterial metabolisms and lactate production of infiltrating neutrophils and macrophages at the inflammatory foci (Park and Kim, 2013). For example, pleural effusions are frequently found in patients with acute bacterial pneumonia caused by *S. pneumoniae*, with reports of pH values close to 6.8 (Light et al., 1980). In addition, the brain interstitial pH has been observed to decrease to 6.8 in purulent experimental meningitis of *S. pneumoniae*-infected rabbits (Andersen et al., 1989). Notably, the lowest pH value that *S. pneumoniae* has been shown to be tolerant to is around 4.4 in phagosomal vesicles during the first minutes after phagocytosis (Bassoe and Bjerknes, 1985). Moreover, it was demonstrated that *S. pneumoniae* was able to live several hours in endothelial cells in a survival test using extracellular antibiotics (Gradstedt et al., 2013).

Many bacteria are able to survive acidic conditions using different strategies. One of the most relevant mechanisms in streptococci is the extrusion of protons from the cytoplasm by a proton pump, known as F_0F_1-ATPase. The F_0 complex, comprised of subunits *a*, *b* and *c*, is associated to the membrane and has a proton-translocating

* Corresponding author. Tel.: +54 351 4344973x112; fax: +54 351 4333048.
E-mail addresses: jeche@fcq.unc.edu.ar, jechenique6@yahoo.com.ar (J. Echenique).

[1] The three authors contributed equally to this work and the order of these authors is arbitrary.

[2] Current address: Department of Biology, University of Utah, 257 South 1400 East, Room 201, Salt Lake City, UT 84112-0840, USA.

http://dx.doi.org/10.1016/j.ijmm.2014.12.002
1438-4221/

activity that allows this enzyme to act as a proton pump. However, this is not the only mechanism responsible for bacterial survival under acidic conditions. In fact, it has been proposed that the acidic stress response is a combination of various strategies, such as removal of protons, alkalinization of the external environment, expression of chaperones and proteases, DNA repair mechanisms and the participation of signal transduction systems to regulate gene expression (Cotter and Hill, 2003).

Some bacterial pathogens are able to survive under acidic conditions by a mechanism termed acid tolerance response (ATR), a phenomenon whereby the tolerance of an organism to lethal pH increases as a consequence of a prior exposure to a sublethal pH (Cotter and Hill, 2003). In order to survive intracellularly, bacterial pathogens have to resist the acidic environments encountered during the phagocytosis or endocytosis processes in macrophages or epithelial cells, respectively, with the phagosomal pH being low (pH 4.5–5.5) due to the activity of the vacuolar ATPase. For example, *Listeria monocytogenes* is an intracellular pathogen that is able to survive acidic stress by ATR induction. Acid-adapted cells were shown to have a nine-fold increase in invasion efficiency in the enterocyte-like cell line Caco-2 and in J774.A1 macrophages compared with non-adapted cells (Conte et al., 2000). Related to this, it was suggested that the capacity to invade Caco-2 cells depends on ATR induction (Werbrouck et al., 2009). Recently, it was reported that an acid shock (pH 5.0) caused a twelve-fold increase in the number of *L. monocytogenes* inside Caco-2 epithelial cells (Neuhaus et al., 2013).

An ATR mechanism was also reported in *S. pneumoniae*, showing that a subpopulation of pneumococci was able to survive a lethal pH of 4.4 when log phase cells of strain R6 were previously incubated at pH 5.9 (Martin-Galiano et al., 2005). For cells incubated directly at pH 4.4, the survival rate was 10^{-4}, but cells pre-incubated for 2 h prior to lethal pH had a ten-fold increase in the survival rate. In addition, these authors also demonstrated by microarray assays that adaptation to acidic stress altered the expression of 126 genes, suggesting that this stress response is complex and involves different cellular processes, such as protein fate and the transport of manganese and iron.

In our laboratory, we described that acidic stress was also capable of inducing autolysis in *S. pneumoniae* when incubated for more than one hour at pH 5.9 (Pinas et al., 2008), and named this process acidic-stress induced lysis (or ASIL). In *S. pneumoniae*, autolysis is executed mainly by the major autolysin LytA. Acidic stress may represent for *S. pneumoniae* an alternative condition, in addition to competence and antibiotics, to assure the release by autolysis of DNA, cell wall compounds and virulence factors.

It has been described that autolysis is triggered by competence development at pH 7.8 and regulated by the two-component system ComDE (Claverys et al., 2009). The LytA autolysin is encoded by the *lytA* gene and located in the same operon as *recA*. The latter encodes a protein responsible for the homologous recombination of exogenous DNA, which belongs to the *cinA-recA-dinF-lytA* operon and is regulated by ComDE during competence development. Briefly, this TCS senses a competence-stimulating peptide (CSP) and behaves as a quorum sensing mechanism (Mortier-Barriere et al., 1998), with CSP being a pheromone derived from a precursor, ComC, which is processed and exported by the ABC transporter ComAB. It is assumed that a critical concentration of extracellular CSP is sensed by its receptor, the ComD histidine kinase, thereby leading to autophosphorylation. The transfer of the phosphate group activates ComE, its cognate response regulator, inducing the expression of *comCDE* and several other genes, such as *comX*. This gene codes for ComX (Claverys et al., 2006), a competence-specific sigma factor that induces the transcription of late genes needed for transformation (DNA uptake and recombination), such as the *cinA-recA-dinF-lytA* operon.

The ComDE-controlled regulatory circuit that leads to competence development takes place under the slightly alkaline pH of 7.8. In contrast, we reported that acidic stress triggers LytA-mediated autolysis, and curiously, this phenomenon was regulated by a CSP-independent ComE pathway, in which ComE did not require ComD phosphorylation to trigger autolysis at pH 5.9. We also investigated CiaRH, a TCS that participates in the early control of competence induction, cefotaxime resistance, stress response and virulence (Echenique et al., 2000; Giammarinaro et al., 1999; Pinas et al., 2008). Under acidic conditions, the *null* ciaR mutant showed accelerated autolysis, with the analysis of *ciaR comE* double mutants revealing that CiaRH protects cells from ASIL by a ComE-independent pathway (Pinas et al., 2008). We proposed that ComE is the principal route of the signaling pathway that determines a global stress response. Considering that the same type of stress provokes the induction of autolysis and the acid-tolerance response, we investigated the possible contribution of the pneumococcal F_0F_1-ATPase, the putative signaling systems that may control these contrasting mechanisms and their impact on the intracellular survival when infecting pneumocytes or macrophages. Here, we demonstrated the relevance of F_0F_1-ATPase as well as the TCSs ComDE and CiaRH in the control of the antagonistic processes ATR and ASIL, both in vitro and in tissue cultures, where bacterial cells must overcome the acidic pH in endosomes in order to survive or to induce autolysis and die. This is the first report on TCSs that control a stress response and decide between a survival and a suicide mechanism.

Materials and methods

Bacterial strains, growth and transformation conditions

All strains used in this study and their relevant characteristics are listed in Supplementary material (Table S1). The growth conditions and stock preparation for pneumococcal and *Escherichia coli* strains have been reported elsewhere (Pinas et al., 2008), and the transformation assays have also been previously described (Albarracin Orio et al., 2011; Echenique et al., 2000).

Cell lines and culture conditions

Human lung epithelial carcinoma (A549) and murine macrophage (RAW264.7) cell lines were cultured at 37 °C, 5% CO_2 in Dulbecco's modified Eagle medium (DMEM) with 4.5 g/l of glucose and 10% of heat-inactivated fetal bovine serum (FBS) (Gibco BRL, Gaithersburg, Md.). Fully confluent A549 or RAW264.7 cells were split once every two or three days via trypsin/EDTA treatment and diluted in fresh media before being cultivated in Filter cap cell flasks 75 cm^2 (Greiner Bio-one no. 658175) until passage 6.

Acid tolerance response assays

ATR experiments were carried out in THYE medium (30 g/l Todd-Hewitt, 5 g/l yeast extract). Prior to sterilization the pH was adjusted to pH 7.8 (with 1 N NaOH) or to pH 5.9 and 4.4 (with 10 N HCl). To determine survival to a lethal pH of 4.4 under non-acid-induced conditions, the pneumococcal strains were first grown at 37 °C in THYE (pH 7.8). When cultures reached $OD_{600\,nm} \sim 0.3$, 100 μl aliquots were taken and added to 900 μl of THYE (pH 4.4) and incubated for 2 h at 37 °C. Then, serial dilutions were made in THYE (pH 7.8) and plated onto 5% of sheep blood tryptic-soy agar (TSA) plates. After 48 h of incubation at 37 °C, colonies were counted to determine the number of survivors, with the total CFU being obtained by plating serial dilutions of cells grown THYE pH 7.8 onto 5% sheep blood TSA, made just before being switched

the cells to pH 4.4. In parallel, to determine survival under acid-induced conditions, bacterial cells were grown in THYE (pH 7.8) until $OD_{600\,nm} \sim 0.3$, centrifuged at 8000 × *g* for 5 min, resuspended in THYE (pH 5.9) and incubated for 2 h at 37 °C (adaptation period). Culture aliquots were taken and serially diluted in THYE pH 7.8 for total cell counting, while other aliquots were diluted ten times in THYE (pH 4.4) and incubated for 2 h at 37 °C to determine the survival percentage as described above. For both assays (acid-induced and non acid-induced conditions), this was calculated by dividing the number of survivors at pH 4.4 by the number of total cells at time zero (before incubation at pH 4.4). For ATR experiments done in presence of F_0F_1-ATPase inhibitors, optochin was added at subinhibitory concentrations of 3.0 μM (optochin MIC 5.0 μM), and DCCD was also added at subinhibitory concentrations of 100 μM (DCCD MIC 500 μM). Data were expressed as the mean percentage ± standard deviation (SD) of independent experiments performed in triplicate. MIC, minimal inhibitory concentration.

ASIL assays

The ASIL protocol was performed as described elsewhere (Pinas et al., 2008), except that THYE medium was used instead of Acetate Basic Medium (ABM). The THYE medium was adjusted to pH 7.8 with 10 N NaOH or to pH 5.9 with 10 N HCl, and after autoclaving, glucose was added to a final concentration of 0.4%. Data were expressed as the mean percentage ± SD of independent experiments performed in triplicate.

Intracellular survival assays

The number of recovered viable intracellular pneumococci after endocytosis or phagocytosis was quantified by a modified antibiotic protection assay (Fig. S1). Briefly, 3.2×10^5 of A549 cells or 4.2×10^5 of RAW264.7 cells per well were seeded in 6 well plates (Greiner Bio-One657160) and cultured in DMEM supplemented with 20% of fetal bovine serum (FBS) and incubated for 12 h. Streptococci were grown in THYE to mid-log phase ($OD_{600\,nm}$ 0.3) and resuspended in DMEM (with 20% FBS). Infection of cell monolayers was carried out using a multiplicity of infection (MOI) 20:1. Bacterial internalization after incubation and washes with extracellular antibiotics was approximately 1%, and the occurrence of apoptosis/necrosis caused by pneumococcal infection quantified by flow cytometry (annexin V/propidium iodide labelling kit; Invitrogen) was approximately 5–10% in all time points analyzed (data not shown). Incubation time was dependent on the cell line infected, being 3 h for A549 and 1 h for RAW264.7 cells. After this infection period, cells were washed thrice with phosphate-buffered saline (PBS) and fresh DMEM (without FBS) containing 150 μg/ml potassium penicillin G (Sigma P7794) and 900 μg/ml gentamicin sulphate (US Biological G2030). After a 20 min rest period, cells were washed thrice with PBS. The eukaryotic cells were lysed by centrifugation for 5 min at 10,000 rpm and the bacterial pellet was resuspended in THYE medium. The number of internalized bacteria at different time points was quantified after serial dilutions and plating on BHI 5% sheep blood agar plates with incubation for 16 h at 37 °C. The time scale referred to the time after elimination of the extracellular bacteria by antibiotic treatment.

A 100% survival was set after 20 min of antibiotic treatment (Fig. S1), and all the samples were referred to this point to calculate the respective percentages.

Construction of insertion–duplication mutants

Insertion–duplication mutagenesis was used to create null mutants in the R801 genetic background. To introduce mutations into the genes that encode the pneumococcal histidine kinases (*hk*) or response regulators (*rr*) in the R801 genetic background, we amplified the internal fragments of the *hk* or *rr* genes described in the genome of *S. pneumoniae* R6 strain with specific primers containing the *Eco*RI or *Bam*HI restriction sites (Table S2) (Tettelin et al., 2001). These PCR products were cloned into the pCR2.1-TOPO vector (Invitrogen, USA), and the *Eco*RI-*Bam*HI DNA fragments liberated from these plasmids were ligated to plasmid pJDC9 (Chen and Morrison, 1987) previously digested with *Eco*RI and *Bam*HI. The resulting constructions were used to transform the R801 strain. Transformants were selected in 5% sheep blood Brain Heart Infusion (BHI) agar plates containing 2.5 μg/ml erythromycin, and the presence of *hk* or *rr* mutations were confirmed by PCR using the respective primers (Table S2). The *comE::km* mutant (RC830) was constructed by transformation of R801 with pPT8-km, as previously described (Echenique et al., 2000). The selection of transformants was performed in 5% sheep blood BHI agar plates supplemented with 250 μg/ml kanamycin. To avoid the selection of putative compensatory mutations, six insertion mutants of each transformation were analyzed, and one of them was selected when all the tested mutants showed identical phenotypes. Cultures of insertion mutants were grown maintaining the antibiotic pressure corresponding to each insertion cassette.

Construction of the $comE^{D58A}$ mutant

The $comE^{D58A}$ mutant (RC831) was obtained by transformation of strain R801 with a 569-bp amplicon generated with primers RcomE-RT and FComE^{58}, the latter carrying the $comE^{D58A}$ mutation, which also resulted in the loss of the *Eco*RV site present in the wild-type *comE* sequence. This amplicon was cloned into the pGEM-T easy vector (Promega), and the resulting DNA construct, pGEM-$comE^{D58A}$, was used to transform R801. Then, 200 colonies were picked, pooled into groups of 5 and grown overnight at 37 °C in 1 ml of THYE, with genomic DNA samples from each pool being extracted by a modified CTAB method (Wilson, 2001). The presence of the desired mutation was detected by PCR using the primers FD58A check and RcomE-RT (Table S2). Once a positive pool was identified, DNA purification and PCR was repeated with individual colonies in order to isolate the mutant strain. Finally, incorporation of the mutation into the chromosome was confirmed by PCR amplification, *Eco*RV digestion and DNA sequencing.

Construction of the bgaA mutant

R801 Δ*bgaA::km* (RCB801), a strain lacking β-galactosidase activity, was obtained by PCR-ligation mutagenesis (Lau et al., 2002). Briefly, two internal *bgaA* DNA fragments of approximately 1 kb, corresponding to the 5′ and 3′ regions, were obtained by PCR with the primers pairs Fbgal1/Rbgal1 and Fbgal2/Rbgal2. Fragments 5′ and 3′ were digested with *Xho*I and *Bam*HI, respectively, and ligated to the kanamycin resistance cassette (*aphaA3* gene) liberated from plasmid pPJ1 (Peeters et al., 1988), that was digested with *Sal*I and *Bgl*II. A ligation mixture consisting of 0.3 μg of each fragment was directly used to transform strain R801, and the selection of mutants was carried out in 5% sheep blood Columbia agar plates supplemented with 250 μg/ml kanamycin. The *bgaA* deletion was confirmed by PCR sequencing and the lack of β-galactosidase activity.

Construction of the atpC-lacZ reporter

To study the activity of the *atpC* gene promoter, which encodes for subunit *c* of F_0F_1-ATPase (*atpC*), the 242-bp fragment upstream the translational initiation site (bases −242 to −1) was amplified with primers FatpC/RatpC and cloned into pEVP3 digested with *Xho*I–*Xba*I (Claverys et al., 1995), which is a *lacZ* reporter vector

created for insertion–duplication mutagenesis Plasmid pEVP3-*atpC-lacZ*, containing the *atpC::lacZ* transcriptional fusion, was used to transform the Δ*bgaA::km* mutant to integrate this construction into the pneumococcal chromosome, and the selection of transformants was carried out in 5% sheep blood-Columbia agar supplemented with 2 μg/ml chloramphenicol. The presence of the mutation was confirmed by PCR and DNA sequencing.

Determination of β-galactosidase activity

The β-galactosidase activity in pneumococcal strains was determined as described (Halfmann et al., 2007a) with modifications. Bacterial cells were cultured into the THYE medium until cell density reached the mid-log growth phase ($OD_{600\,nm} \sim 0.3$), centrifuged at 10,000 × *g* for 10 min, resuspended in Z-buffer (Halfmann et al., 2007a), and lysed by the addition of lysozyme to a final concentration of 1 mg/ml with incubation for 60 min at 37 °C. The cell suspensions were sonicated (Vibra-Cell™; Sonics) at 70% power with 4 pulses of 30 s each (waiting 30 s between pulses) on ice. Bacterial lysates were kept in ice, and the β-galactosidase activity was determined using 0.8 mg/ml *o*-nitro-phenol-β-D-galactopyranoside (ONPG, Sigma) at 37 °C with the release of nitrophenol being followed spectrophotometrically at 420 nm for 60 min. Specific β-galactosidase activity was expressed as nanomoles of nitrophenol released per minute per mg of protein, and protein concentration was determined by the method of Bradford, using the Bio-Rad protein assay kit.

Deoxycholate-induced autolysis

Detergent-induced autolysis was used to determine probable changes in LytA expression during acidic stress exposure. Deoxycholate (DOC), a known inducer of autolysis, was used in these assays after acidic exposure, as described (Mellroth et al., 2012). The *comA* mutant was used as "wild-type" strain to avoid LytA expression by competence development at pH 7.8, and the *lytA* mutant was used as negative control. These strains were cultured in THYE medium (pH 7.8) until an $OD_{600\,nm}$ of 0.3, centrifuged, resuspended in a same volume of THYE medium (pH 5.9) and incubated at 37 °C for 1 h for a potential acidic induction of LytA. After that, DOC was added (0.05, 0.075 and 0.1%) to induce autolysis, and optical density was determined at $OD_{600\,nm}$ at different time points.

Bioassay to determine LytA activity on the pneumococcal surface

To determine LytA activity on the surface of *S. pneumoniae* mutants, we designed a bioassay based in the co-cultivation of different strains. For this assay, we choose the *lytA* mutant (a streptomycin-resistant variant) as Sm^R non-autolytic tester cells (hereafter tester cells) (Table S1), which will be able to lyse only when they contact cells that express LytA on their surface or release it to the medium. To determine autolysis induced by acidic stress exclusively, the *comA* mutant was used as "wild-type" strain to avoid LytA expression via competence development. We used the *comE comA*, and *ciaR comA* double mutants to determine the impact of ComE and CiaR on extracellular LytA expression. All strains were grown in THYE until $OD_{600\,nm}$ 0.3, and the *comA* and the double mutants were independently co-incubated with the tester cells (keeping a ratio of 3 LytA-expressing cells/1 tester cell) at different time points in THYE pH 5.9, and cell suspensions were plated onto 5% sheep blood tryptic-soy agar (TSA) plates containing 200 μg/ml of streptomycin. The percentage of lysis of tester cells was calculated as following: [100 − % of survival tester cells (Sm^R UFC/initial Sm^R UFC × 100), considering that this strain mainly dies by lysis.

Fluorescence microscopy

RAW264.7 macrophages were seeded on glass coverslips in 24-well plates overnight. Infection was carried out as described above. Then, after infection, the macrophages were washed thrice with PBS and fixed with 4% paraformaldehyde for 10 min. Cells were incubated 10 min with quenching solution (10 mM NH_4Cl), washed with PBS, and permeabilized with 0.1% Triton X-100/PBS for 7 min. Blockage was made using GS (Goat serum 2.5% from Invitrogen in 0,1% Triton X-100/PBS) for 5 min, followed by FSG (gelatin from cold water fish skin 0.4% from Sigma in 0.1% Triton X-100/PBS) for 5 min. Glass coverslips were washed with 0.2% Tween/PBS and incubated for 18 h at 4 °C with Rabbit polyclonal antibody to Rab7 (Abcam, Ab74906, 1/500 dilution in FSG) and with Mouse monoclonal antibody to TEPC15 (anti-phosphoryl-choline from bacterial cell wall from Sigma, M1421; 1/200 dilution in FSG). After three washes with 0.2% Tween/PBS, the cells were blocked with FSG for 5 min followed by GS for 5 min, before being incubated for 30 min at 37 °C with Goat Anti Rabbit Alexa Fluor 594 (Invitrogen, A11072) in GS and Goat Anti Mouse Alexa Fluor 488 (Invitrogen, A11017), both at a dilution of 1/800 in GS. After a final washing step, glass coverslips were mounted using Mowiol 4-88 (Sigma, 81381). An analysis was carried out using a confocal laser-scanning microscope (Olympus FV300) with a 100× oil immersion lens.

Statistical analysis

The data reported in the figures are expressed as means ± standard deviations (SD), which are representative of at least three independent experiments. The ANOVA and *t*-Student statistical tests were performed using GraphPad Prism version 5.00 for Windows, GraphPad Software, San Diego, California, USA. Statistical significant differences are indicated; $p < 0.001$ ***, $p < 0.01$ **, $p < 0.05$ *.

Results

F_0F_1-ATPase is involved in the ATR and ASIL mechanisms

In our laboratory, the R801 wild-type strain was able to develop acid tolerance response (ATR) at mid-log phase ($OD_{600\,nm}$ 0.3) during the first 2 h of incubation at pH 5.9, using the same culture conditions as those described previously for the pneumococcal R6 strain (Martin-Galiano et al., 2005) (Fig. 1A). As mentioned earlier, some bacterial species display an ATR mechanism under acidic conditions that allow bacterial cells to survive to lethal pH when they are previously exposed to sublethal pH (Cotter and Hill, 2003), with F_0F_1-ATPase playing a leading role in ATR development. With the purpose of determining the contribution of this enzyme to the ATR of *wt* and *atpC* mutants, we utilized classical inhibitors of F_0F_1-ATPases, such as *N,N′*-dicyclohexylcarbodiimide (or DCCD) (Molenaar et al., 1992) and optochin (Fenoll et al., 1994) at subinhibitory concentrations, 3 μM of optochin (MIC_{opt} 5 μM for *wt*; MIC_{opt} 80-160 μM for *atpC* mutants) and 100 μM of DCCD (MIC_{DCCD} 500 μM for *wt* and *atpC* mutants). These subinhibitory concentrations of optochin and DCCD did not affect the normal growth of *wt* and *atp* mutants in standard culture media like THYE (data not shown). When ATR was determined in the *wt* strain incubated with optochin or DCCD during ATR induction at pH 5.9, a decrease in survival to lethal pH of approximately 60 and 80% was observed, respectively, compared with non-inhibitor conditions (Fig. 1A), suggesting that F_0F_1-ATPase was involved in this mechanism.

In *S. pneumoniae*, the complex F_0 of F_0F_1-ATPase is comprised of the subunits *a*, *b* and *c*, which are encoded by the *atpA*, *atpB* and *atpC* genes, respectively (Fenoll et al., 1994). This enzyme is essential

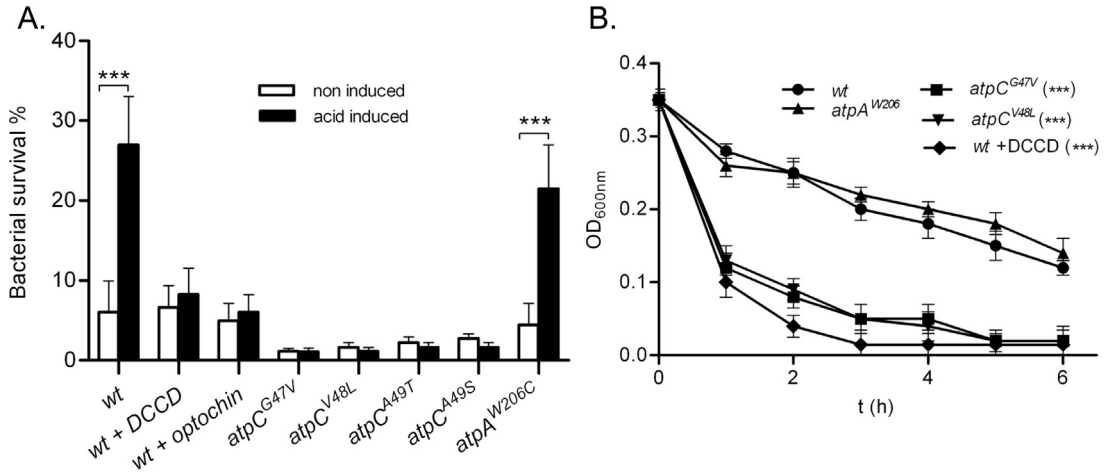

Fig. 1. F_0F_1-ATPase is involved in the acid stress response. (A) Acid tolerance response (ATR) was determined in *wt* and its respective *atpAC* mutants. Treatment with F_0F_1-ATPase inhibitors (3 μM optochin or 100 μM DCCD) is only shown for *wt*. To determine the survival percentage of *wt* and *atpAC* strains, cells were incubated for 2 h at pH 4.4 in THYE medium. The non-induced cells (white bars) were directly exposed for 2 h at pH 4.4, whereas, the acid-induced cells (black bars) were previously incubated for 2 h at pH 5.9 and then at pH 4.4 in THYE medium. Statistical significance was determined by two-way ANOVA with a Bonferroni posttest, and significant differences are indicated by: *** $p < 0.001$. (B) Acid-stress induced lysis (ASIL) was determined in *wt* and its respective *atpAC* mutants. Strains *wt* (circles), $atpA^{W206C}$ (up triangles), $atpC^{G47C}$ (squares), $atpC^{V48L}$ (down triangles), *wt* treated with 100 μM DCCD (diamonds) were grown in THYE medium at pH 7.8, centrifuged and resuspended in THYE medium at pH 5.9 at 37 °C, and lysis was followed by loss of turbidity at $OD_{600\,nm}$. The *wt* cells treated with 3 μM optochin showed a similar phenotype to that revealed by DCCD treatment (data not shown). The $atpC^{A49T}$ and $atpC^{A49S}$ showed the same phenotype that $atpC^{G47V}$ and $atpC^{V48L}$ (data not shown). Data are representative of at least three independent experiments. Statistical significance was determined by one-way ANOVA with a Bonferroni posttest, and significant differences are indicated by: *** $p < 0.001$.

for *S. pneumoniae* (Ferrandiz and de la Campa, 2002), what complicates genetic studies. Thus, we decided to use point mutations in the *atpAC* genes (there are not *atpB* mutations described so far) that conferred optochin resistance without any growth alterations compared with *wt*, which were isolated from clinical strains and transformed into the R801 laboratory strain (Cortes et al., 2008). By homology with the F_0F_1-ATPase of *Escherichia coli*, the *atpC* mutations that confer optochin resistance are located near aspartate 52 that stabilize the *c*-subunit structure, and they could be altering the H^+ translocation of *S. pneumoniae* (Pikis et al., 2001). In this sense, when the ATR phenotype was analyzed, all the *atpC* mutants ($atpC^{G47V}$, $atpC^{V48L}$, $atpC^{A49T}$ and $atpC^{A49S}$) not only showed reduced ATR (Fig. 1A), but were also more sensitive to pH values between 5.6 and 4.4 without a previous incubation to sublethal pH 5.9 (data not shown). In contrast, the $atpA^{W206C}$ mutant had an ATR phenotype comparable to *wt*, indicating that the subunit *c* of F_0F_1-ATPase was involved in ATR (Fig. 1A).

The ability of these *atpAC* mutants to lyse under acidic conditions (ASIL at pH 5.9) was also evaluated as we described previously (Pinas et al., 2008), with the $atpA^{W206C}$ mutant displaying the same autolytic behavior as *wt*. However, the four *atpC* mutants ($atpC^{G47V}$, $atpC^{V48L}$, $atpC^{A49T}$ and $atpC^{A49S}$) showed an accelerated autolysis compared with *wt* (Fig. 1B), implying that these *atpC* mutants probably underwent a rapid intracellular acidification under acidic conditions due to an altered F_0F_1-ATPase activity, as suggested by Pikis et al. (2001), that led cells to autolysis earlier than *wt*. These *atpAC* mutations were also transferred to the capsulated D39 strain (serotype 2; NCTC 7466) (Williams et al., 2007), and the ATR and ASIL phenotypes of their respective mutants were similar to the R801 strain (Fig. S2).

F_0F_1-ATPase promotes survival of S. pneumoniae in RAW264.7 macrophages

When *S. pneumoniae* is endocytosed by epithelial cells, pneumococci are usually eliminated by the endocytic pathway in the lysosomal compartment (Radin et al., 2005). Related to this, we found that this pathogen was able to survive several hours inside A549 pneumocytes (type II) or macrophages RAW 267.4, suggesting that *S. pneumoniae* could tolerate the acidic pH of endosomes or phagosomes as a result of ATR induction. For this reason, we decided to evaluate whether F_0F_1-ATPase was involved in this survival mechanism, using monolayers of A549 pneumocytes and RAW264.7 macrophages in multiwell plates which had been infected with *wt* or *atpAC* mutants at a pneumococci/cells ratio of 20:1. To obtain similar amounts of internalized pneumococci in both cell models, incubation was performed for 1 h for macrophages and 3 h for pneumocytes. Cells were then washed, incubated with extracellular antibiotics to kill bacterial cells that were not endocytosed or phagocyted (protection assays), and lysed without altering the pneumococcal viability. Samples were then cultured on blood agar plates in order to count the bacterial viable cells. For this assay, we only considered results obtained from macrophages, because pneumocytes showed a very low uptake of *atpAC* mutants (data not shown). Consequently, we used RAW264.7 macrophages, where the internalization of pneumococci was optimal for our purpose. *S. pneumoniae* follows the classical endocytic pathway as shown by co-localization with Rab7, a late endocytic pathway marker, as described elsewhere (Radin et al., 2005). Pneumococci are intracellularly located and potentially inside vesicles (Fig. 2A). At time zero (after incubation of 1 h at 37 °C, see infection scheme in Fig. S1), pneumococci internalization was similar for *wt* and *atpAC* mutants, and it was approximately 1%. However, after another hour of incubation, $atpA^{W206C}$ showed no alteration in its survival capacity, whereas the $atpC^{G47V}$ and $atpC^{A49T}$ mutants revealed a decrease in bacterial viability of 40–60% compared with *wt* (Fig. 2B), displaying also a decrease as observed by ATR assays, although bacterial survival was more reduced than in macrophages (Fig. 1A). These results indicate that F_0F_1-ATPase, probably mediating ATR, allowed *S. pneumoniae* to survive inside macrophages.

ATR induction does not depend on ASIL development

We previously described that autolysis is induced in pneumococci grown at log-phase rates when incubated at pH 5.9 after 1 h (ASIL), with cell lysis being produced by the enzymatic activity of the major autolysin LytA (Pinas et al., 2008). These contrasting responses between ATR and ASIL, caused by the same stress

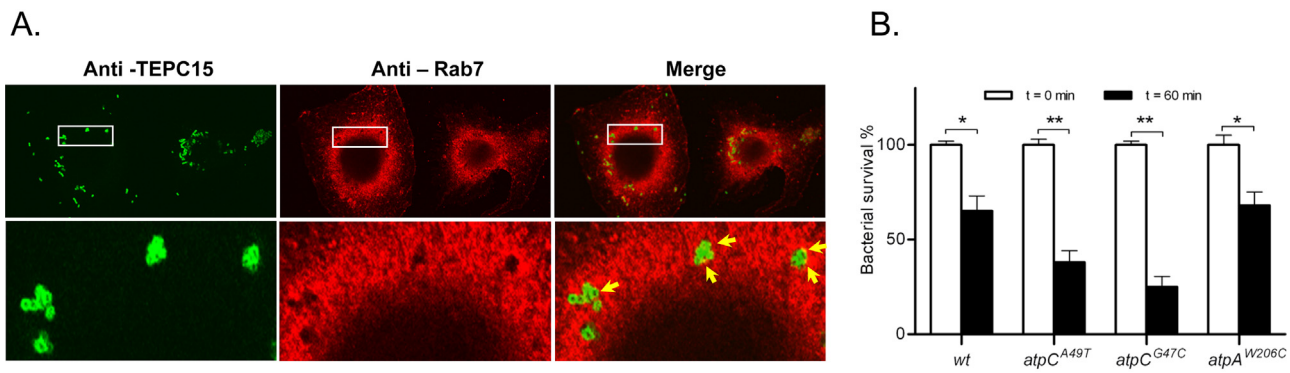

Fig. 2. *S. pneumoniae* resides in an intracellular compartment and needs F_0F_1-ATPase to survive in RAW 264.7 macrophages. (A) After 60 min of infection with strain R801 (*wt*) and extracellular antibiotic treatment, the intracellular pneumococci were stained with the monoclonal antibody anti-phosphoryl-choline (anti-TEPC-15) followed by Alexa Fluor 488 antibody (green). As an intracellular marker, Rab7 vesicles were stained using a polyclonal antibody anti-Rab7 labeled with Alexa Fluor 594 (red). Details of the pictures showing *S. pneumoniae* and Rab7 markers are presented in the lower panel. (B) The relative survival of *wt* and *atpAC* mutants in RAW 264.7 macrophages was compared using a classical protection assay. Pneumococci grown to mid-log phase were incubated at a bacteria:macrophage ratio of 20:1 for 1 h. After antibiotic treatment, surviving pneumococci were determined by plating on BHI agar blood for 16 h. Survival percentages were calculated by considering the total amount of internalized bacteria obtained at time zero after antibiotic treatment. Data are representative of at least three independent experiments. Statistical significance was determined by two-way ANOVA with a Bonferroni posttest, and significant differences are indicated by: * $p < 0.05$; ** $p < 0.01$. (For interpretation of the references to color in this figure legend, the reader is referred to the web version of this article.)

condition, led us to analyze whether a strain deficient in autolysin (*lytA* mutant), which was incapable of lysing under acidic stress, could favor the induction of ATR. For this purpose, the same amount of *wt* and *lytA* cells grown to mid-log phase was independently incubated at pH 5.9 for 2 h at 37 °C followed by pH 4.4 for 2 h. On analyzing the ATR phenotype, it was observed that the total cells in the *lytA* mutant increased 2.9 times compared with *wt* during the adaptation period at pH 5.9. Although the *lytA* strain had an increased number of total cells after acid exposure because autolysis was blocked, this mutant induced the same amount of acid tolerant cells compared with the *wt* strain (Fig. 3A). For that reason the survival percentage of both acid-induced and non-induced conditions showed no significant differences (Fig. 3B).

To explain the acid-induced phenotype showed by the *lytA* mutant, we cannot discard the possibility that a basal level of autolysis occurs in all cells exposed to acidic stress, and inactivation of *lytA* may increase the overall CFU of acid-tolerant and lytic cells, but not proportionally. Another possibility is the existence of two subpopulations that respond to acidic stress, one undergoing ATR to survive, and another one opting for autolysis. Thus, our results indicate that ATR induction does not depend independent of ASIL development.

A screening of TCS mutants showed that ComE and CiaR regulate ATR and ASIL

Given that bacteria generally sense environmental stimulus through signal transduction systems, we evaluated the contribution of the two-component systems (TCS) to acidic stress response of *S. pneumoniae*. For this purpose, we constructed insertion mutants of all the histidine kinase genes that belong to the 13 TCSs found in the pneumococcal genome, and also that of the *ritR* gene that encodes an orphan response regulator (Tettelin et al., 2001). As we could not obtain the *hk12* (or *comD*) mutant by insertional mutagenesis, we constructed *comD*^{F163X}, which contains a stop codon at Phe-163 that generates a truncated and inactive form of ComD.

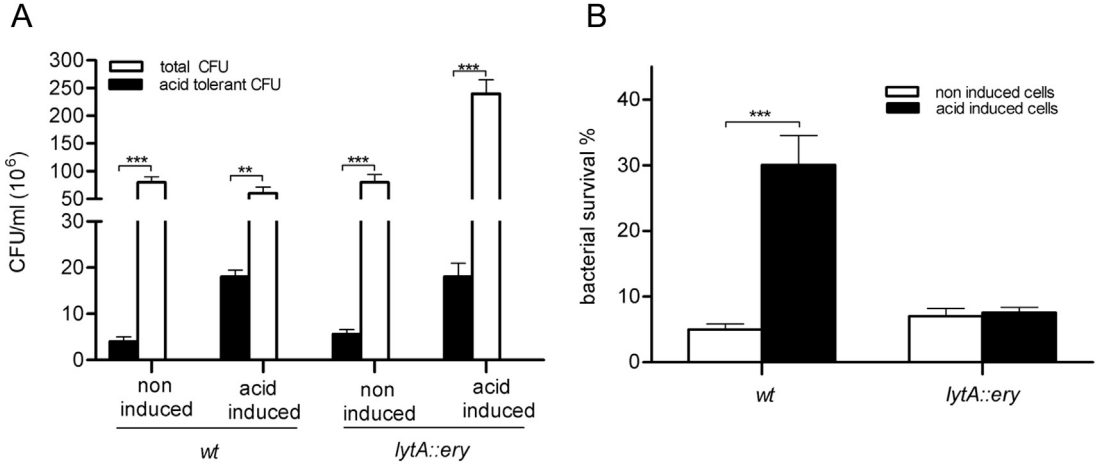

Fig. 3. Blocked autolysis does not modify the induction of acid tolerant cells. (A) ATR was evaluated in *wt* and the *lytA* mutant, and data are expressed as total CFU (colony forming unit) and acid tolerant CFU. The acid-induced cells were incubated for 2 h at pH 5.9 in THYE medium and compared with the non-induced cells. The total cells (white bars) and acid tolerant cells (black bars) are shown, and they correspond to the amount of cells before and after the incubation at pH 4.4, respectively, subsequent to the pH 5.9 induction when indicated. In the *lytA* mutant induced by acidic pH, the acid tolerant cells were similar to the *wt* strain, in spite of the higher number of total cells being caused by blocked autolysis. (B) The same data of ATR assays showed in panel A is expressed as percentage values (acid tolerant CFU/total CFU × 100). Data are representative of at least three independent experiments. For both panels, statistical significance was determined by two-way ANOVA with a Bonferroni posttest, and significant differences are indicated by: ** $p < 0.01$; *** $p < 0.001$.

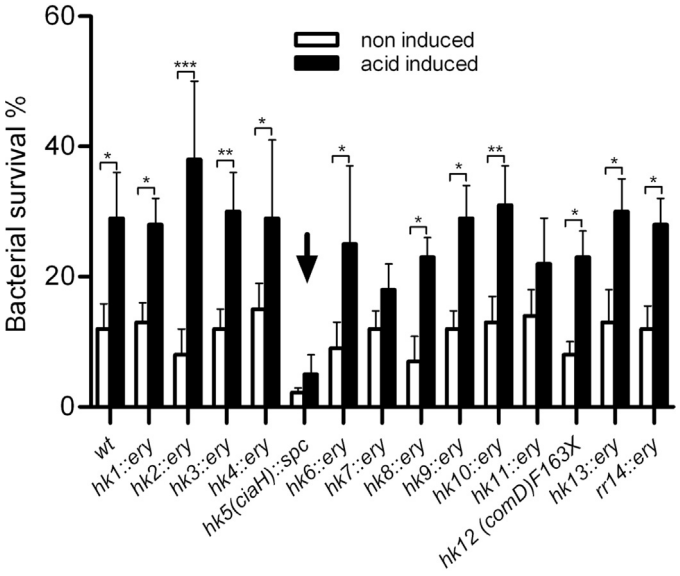

Fig. 4. Contribution of two-component systems to the ATR mechanism. ATR was determined in *wt*, *hk and rr* mutants (*hk* are genes encoding for histidine kinases and *rr* are genes encoding for response regulators, which belong to the two-component systems described in the genome of *S. pneumoniae*) as mentioned in the Material and methods section. The acid-induced cells were incubated for 2 h at pH 5.9 in THYE medium and compared with the non-induced cells. Arrow indicates a decreased ATR showed by *ciaH::spc*. Data are representative of at least three independent experiments. Statistical significance was determined by two-way ANOVA with a Bonferroni posttest, and significant differences are indicated by: * $p < 0.05$; ** $p < 0.01$; *** $p < 0.001$. References obtained from the R6 genome (http://genolist.pasteur.fr/StreptoPneumoList/index.html): *hk01* (spr1473); *hk02* (spr1226, *micA*, *vicK*); *hk03* (spr0343); *hk04* (spr1894; *phoS*); *hk05* (spr0708, *ciaH*); *hk06* (spr1997); *hk07* (spr0153); *hk08* (spr0077); *hk09* (spr0579); *hk10* (spr0529, *vncS*); *hk11* (spr1815); *hk12* (spr2042, *comD*); *hk13* (spr0464); *rr14* (spr0336, *ritR*).

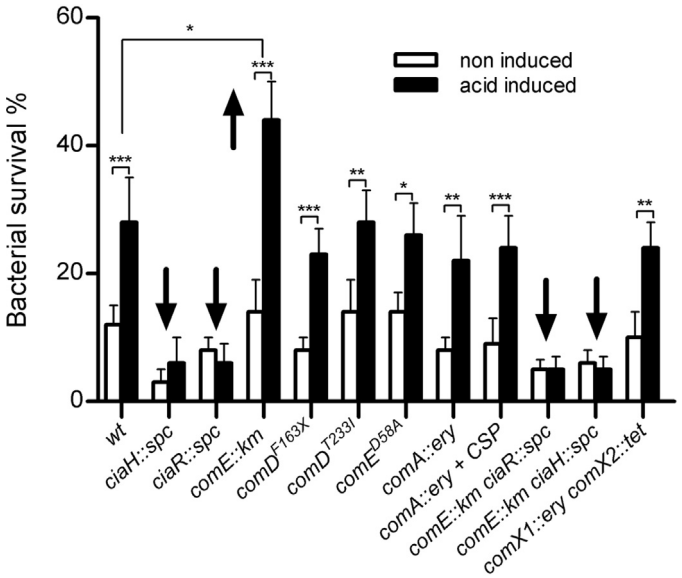

Fig. 5. Analysis of the role of *com* and *cia* mutants on ATR development. ATR was determined in the *com* and *cia* mutants and the *wt* strain. The *comA* mutant was also treated with 20 nM CSP. The acid-induced cells (black bars) were incubated for 2 h at pH 5.9 in THYE medium and compared with the non-induced cells (white bars). The *wt* data is the same than that showed in Fig. 4. Data are representative of at least three independent experiments. Statistical significance was determined by two-way ANOVA with a Bonferroni posttest, and significant differences are indicated by: * $p < 0.05$; ** $p < 0.01$; *** $p < 0.001$.

This mutant, which lacks the kinase domain, had no effect on the transcription of the *comCDE* operon and had normal ComE expression (Martin et al., 2000; Pinas et al., 2008). The ability of these TCS mutants to induce ATR was analyzed and compared with *wt*. We found that *ciaH::spc* displayed a six-fold decreased survival rate under acidic stress conditions compared with *wt* (Fig. 4). Moreover, when the *ciaR::spc* mutant (*ciaR* encodes for the cognate response regulator of CiaH) was evaluated, the results were identical to those observed for the *ciaH::spc* mutant (Fig. 5). Because the *ciaRH* genes constitutes an operon, the *ciaR::spc* mutant has polar effect on *ciaH*, so this mutant should be considered as double mutant. Continuing with the ComDE pathway analysis, although *comD*^{F163X} showed an ATR similar to *wt*, we wondered about a putative participation of ComE in the induction of this mechanism. As mentioned before, we reported that ComE was essential to induce autolysis under acidic conditions (or ASIL) without the participation of its cognate histidine kinase, ComD, or its associated quorum-sensing mechanism that involves CSP during competence development at pH 7.8 (Pinas et al., 2008). Recently, it was demonstrated that the ComE^{D58E} mutant mimics the phosphorylated state of ComE. This mutant is able to dimerize and to activate competence as well as ComE phosphorylated by ComD, in contrast with the unphosphorylatable ComE^{D58A} mutant. The authors proposed that the phosphorylation by ComD activates ComE by favoring its dimeric configuration (Boudes et al., 2014).

Considering that CiaRH and ComE are involved in both competence and ASIL (Dagkessamanskaia et al., 2004; Echenique et al., 2000; Pinas et al., 2008), because CiaR is necessary for ATR induction, we could expect that ComE could participate in the ATR mechanism. Coincidently, we detected a significant increase ($p < 0.05$) in the ATR of the *comE::km* mutant compared to *wt* (Fig. 5). Because the *comCDE* genes constitute an operon in this order, the *comE::km* mutant has not polar effect on the *comD* expression. To test the effect of these mutations in the capsulated D39 strain, we constructed the *comE::km* and *ciaR::spc* strains in this genetic background, and both ATR and ASIL tests were similar to their respective mutants in the R801 strain (Fig. S2), suggesting that acid response is still expressed in capsulated strains of *S. pneumoniae*.

Based on these results, we decided to analyze further the putative contribution of the ComDE system to ATR by genetic approaches, using mutants associated to this signaling mechanism. In addition to *comD*^{F163X}, another *comD* mutant was analyzed, *comD*^{T233I}, which encodes a hyperactive kinase that phosphorylates ComE constitutively thus inducing competence independently of CSP activation (Martin et al., 2000; Pinas et al., 2008). The *comD*^{T233I} mutant displayed an ATR phenotype similar to that shown by *wt* (Fig. 5). Related to this, the *wt* phenotype showed by the *comD*^{F163X} mutant suggested that ComE could not be activated by ComD phosphorylation during ATR induction. To test this, we analyzed the *comE*^{D58A} mutant, which contains a modification in the Asp-58 that is usually phosphorylated by ComD, and is unable to develop competence at pH 7.8, as previously described (Martin et al., 2010). The *comE*^{D58A} mutant presented a similar ATR phenotype to *wt*. All together, these results suggested that ComE controls ATR through a ComD-independent pathway, as it was demonstrated for the ASIL mechanism. In this scenario, it seems that the quorum sensing mechanism known for ComDE is not required for controlling ComE expression in response to acidic stress. To test this hypothesis, we took advantage of the *comA* mutant, unable to secrete the competence-stimulating peptide (CSP) used by ComD to sense cell density, however, *comA* mutants can be complemented by synthetic CSP added externally, as reported in a previous work (Echenique et al., 2000). The *comA* mutant did not change its ATR phenotype when CSP was added during incubation at pH 5.9, with this mutant showing a behavior similar to *wt* (Fig. 5). During ASIL development, regulation by ComE was also independent of ComX, a competence-specific sigma factor that induces the transcription of late genes needed for transformation (Pinas et al., 2008).

We then analyzed ATR in the *comX1::ery* and *comX2::tet* double mutant, revealing a phenotype similar to *wt* (Fig. 5). These data confirmed the assumption that the CSP-triggered quorum sensing is not involved in the ATR regulation of ComE under acidic conditions, and that the acid response state is completely different to the X-state, with respect to competence and other cellular processes (Claverys et al., 2006).

So far, we have shown that ComE and CiaH are involved in the development of ATR. To correlate these results with the increased ATR shown by the *comE* mutant, the *comE ciaR* and *comE ciaH* double mutants were analyzed, with both strains revealing similar ATR phenotypes to those displayed by the *ciaR* or *ciaH* single mutants (Fig. 5). This result allows us to conclude that CiaRH has a predominant effect on ComE function.

F_0F_1-ATPase expression is not regulated by either ComE or CiaRH

To this point, we have demonstrated the relevance of F_0F_1-ATPase in ATR development and showed that the regulatory balance between CiaR and ComE modifies the relationship between ATR and ASIL. With the purpose of determining a possible regulatory role of these TCS on the *atp* genes encoding F_0F_1-ATPase, we used an integrative plasmid in *S. pneumoniae* containing the *atpC* promoter fused to *lacZ*. The β-galactosidase assays were performed using the *bgaA::km* mutant (*bgaA* encodes for the main β-galactosidase in *S. pneumoniae*) to avoid basal enzyme activity. To analyze the contribution of CiaR on *atpC* expression, the *ciaR::spc* mutation was introduced by genetic transformation in the *bgaA::km* mutant containing the *atpCp-lacZ*/pEVP3::*cat* fusion. We could not use *comE::km* to analyze the contribution of ComE to *atpC* expression because it carries the same resistance marker as *bgaA::km*, making impossible to combine these mutations in a new strain. In this case, we chose the $comD^{T233I}$ mutant which (maintains a high *comE* expression level by a constitutive hyperphosphorylation of this histidine kinase), which was sequentially transformed to introduce the *bgaA::km* mutation and the *atpCp-lacZ*/pEVP3::*cat* fusion. After exposure at pH 5.9 for 1 h, the *atpC* promoter activity in *wt* (in fact, the *bgaA::km atpCp-lacZ*/pEVP3::*cat* strain) determined by the β-galactosidase assays increased 2.1 times (Fig. 6), as previously reported by northern and microarray analysis (10). Curiously, in the $comD^{T233I}$ and *ciaR* mutants, the *atpC* transcripts showed the same expression pattern as *wt* strain. These results indicate that high level of ComE found in the $comD^{T233I}$ mutant or the lack of CiaR in the *ciaR::spc* mutant do not regulate *atpC* expression, suggesting that the promoter activity of this gene is regulated by another mechanism.

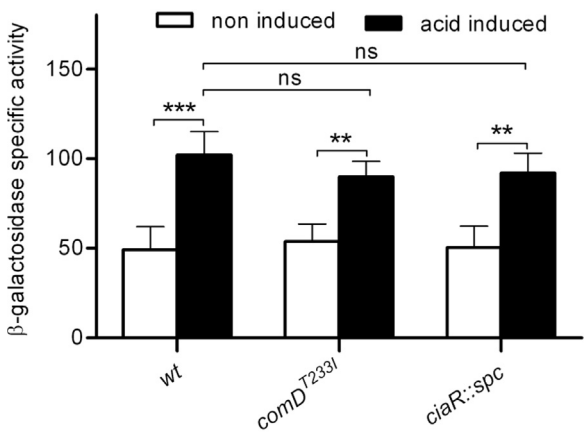

Fig. 6. The transcription of the *atpC* gene is activated by acidic stress but is not regulated by the CiaR and ComE response regulators. Pneumococcal cells were grown at pH 7.8 to exponential phase ($OD_{600\,nm}$ 0.3). The acid-induced cells (black bars) were then incubated for 1 h at pH 5.9 in THYE medium and compared with the non-induced cells (white bars). The β-galactosidase activity was measured in the *wt*, *comE::ery* and *ciaR::spc* strains containing single-copy transcriptional *lacZ* fusions to the structural gene *atpC* (encoding the *c* subunit of the F_0F_1 ATPase) in the *bgaA* strain (lacking β-galactosidase activity). The promoterless *lacZ* gene was integrated as a control for the basal level of reporter gene expression. The units of β-galactosidase activity were described in the Material and methods section. The data shown represent the results of three independent experiments. Statistical significance was determined by two-way ANOVA with a Bonferroni posttest, and significant differences are indicated by: **, $p < 0.01$, ***; $p < 0.001$; ns, not statistically significant.

ComE and CiaR are involved in the expression of the LytA activity on the pneumococcal surface

It was demonstrated by microarray assays that the expression of the *cinA-recA-dinF-lytA* operon did not change during acid exposure (Martin-Galiano et al., 2005), consequently, we suspected that LytA could be modified by acidic stress at translational or post-translational levels. It was shown that a diminution in the production of LytA (produced by a genetic modification in the *cinA-recA-dinF-lytA* operon) caused a delayed autolysis, suggesting that there is a correlation between the total LytA level and the start of autolysis (Mellroth et al., 2012). To determine probable modifications in the LytA level, we analyzed autolysis in acid-induced cells compared with non-induced cells. The *comA* mutant was used as "wild-type" strain to avoid LytA expression via competence development at pH 7.8. Total lysis of acid-induced or non-induced cells was triggered by different concentrations of a known autolytic inducer, deoxycholate (DOC), as described (Mellroth et al., 2012). We observed the same DOC-induced autolytic profile when cells were previously exposed to pH values of 7.8 or 5.9. Different concentrations of DOC showed similar effects, but only data corresponding to the effect of 0.05% DOC is shown (Fig. S4). This result suggested that the LytA level did not change during exposure at acidic conditions.

On the other hand, it was described that the majority of LytA resides in the cytoplasm during exponential phase of growth, and only 5% was associated with the extracellular cell wall (Mellroth et al., 2012). They also demonstrated that the translocation of LytA from cytoplasm to extracellular cell wall caused the onset of autolysis, and that LytA is activated at the substrate level when peptidoglycan biosynthesis is inhibited and not controlled at enzymatic level. Considering this model, our purpose was to investigate the putative cause of lysis induction at pH 5.9, such as the extracellular LytA availability after acidic exposure. To address this point, we designed a bioassay to measure the activity of LytA on the cellular surface of different pneumococcal mutants. As mentioned before, the *comA* mutant was used as the "wild-type" strain to avoid LytA expression via competence development, because we just wanted to determine lysis induced by acidic stress. For this assay, we choose the *lytA* mutant (a streptomycin-resistant variant) as non-autolytic tester cells, which was able to lyse only when contacted other cells that express LytA on their surface. Fig. 8A shows lysis of tester cells caused by extracellular LytA expressed on the surface of different mutants. We observed that the *comA* mutant expressed LytA on its surface when incubated at pH 5.9 and lysed tester cells. As a negative control, we used the *lytA* mutant and it showed no lysis of tester cells (also *lytA* but Sm^S) (Fig. 8A). Regarding the ASIL regulation, the *ciaR comA* mutant showed an increased lysis of tester cells as expected, because the *ciaR* mutant displayed an accelerated ASIL (Pinas et al., 2008) (Fig. 8B). We described previously that the *comE comA* mutant showed a blocked ASIL when exposed at pH 5.9, (Pinas et al., 2008) (Fig. 8B). However, while this mutant was unable to induce autolysis under acidic conditions, it was able to lyse tester cells, displaying extracellular expression of LytA. Altogether, these results suggested that CiaR and ComE control the LytA activity on

the pneumococcal surface, probably regulating the expression of genes that encode essential proteins for the ASIL induction.

CiaR/ComE regulation is relevant for intracellular survival in pneumocytes

Based on results obtained by assays in vitro, we wondered whether this CiaR/ComE regulatory mechanism could be corroborated in a cellular model, where bacterial cells need to survive in the acidic environment of endo/lysosomal compartment. Using a classical protection assay for A549 pneumocytes, we found that a subpopulation of the *wt* cells (25–40%) were able to survive up to 8 h, with the *comE*^{D58A} mutant (non-phosphorylatable by kinase ComD) showing the same behavior. However, the *comE::km* mutant displayed an increase of 2- and 3-fold at 240 and 420 min, respectively, compared with *wt* (Fig. 7A). This intracellular survival increase shown by *comE::km* led us to think that this effect could have been caused by the repression of ASIL or through an ATR increment. Although the *wt* strain should be lysing under the acidic stress imposed by endo/lysosomes, when ASIL is blocked, the *comE::km* mutant displayed an increased survival compared with *wt*. In this context, we decided to block the ASIL mechanism by mutation of the *lytA* gene, which encodes the main autolysin of *S. pneumoniae*, and expected to find the same phenotype as *comE::km*. However, the *lytA* mutant revealed an intracellular survival similar to *wt* (Fig. 7D). In the *lytA* mutant, the subpopulation of pneumococcus that should have lysed under acidic conditions did not induce ATR, as demonstrated by the assays in vitro, and possibly died as result of the acidic shock. In this case, the only survivors belonged to the subpopulation that induced ATR normally in the *wt* cells. Although ASIL was blocked in the *lytA* mutant by elimination of autolysin, ComE and CiaR maintain the control of ATR induction. For this reason, the number of *lytA* survivors found under acidic stress conditions was similar to the *wt* strain. In contrast, and in agreement with ATR assays carried out in vitro, the *ciaR* mutants displayed a notable decrease of −1.6-fold and 6.6-fold at 360 and 420 min, respectively, compared with *wt*, suggesting an activating role of CiaR in ATR development (Fig. 7B). We observed a similar effect in the *comE ciaR* double mutant (Fig. 7C), and it is important to point out that this dominant effect of CiaR on ComE, as demonstrated by ATR assays in vitro, is compatible with and could be extrapolated to the results obtained in a cellular model. These findings provide evidence of the contribution of these TCSs to the survival of *S. pneumoniae* inside eukaryotic cells, being the ATR regulation one of the putative factors involved.

Discussion

S. pneumoniae, in common with other streptococci, lacks a respiratory chain, and is unable to use the F_0F_1 complex for ATP synthesis through oxidative phosphorylation (Konings and Otto, 1983). Consequently, the only function of this enzyme may be to extrude protons from the bacterial cytoplasm under acidic conditions in order to restore intracellular pH. This function demonstrates the relevant role of this enzyme in the response to the acidic stress of *S. pneumoniae*. Related to this, De la Campa's laboratory reported that transcription of the *atp* genes and F_0F_1-ATPase activity increased approximately two-fold as the pH of the medium decreased (Martin-Galiano et al., 2001). In addition, these authors described induction of ATR during the log phase, which augmented at the stationary phase, and performed a transcriptional analysis of the acid tolerance response in strain R6 of *S. pneumoniae*, describing 126 genes that responded to an acidic pH of 6.0, with the *atpC* gene showing a 1.6-fold increase (Martin-Galiano et al., 2005). We obtained similar results from β-galactosidase reporter assays using an *atpC-lacZ* fusion (Fig. 6). However, a direct genetic analysis to test if F_0F_1-ATPase is involved on ATR development has not been performed in *S. pneumoniae*, because the *atp* operon is essential for the viability of *S. pneumoniae* (Ferrandiz and de la Campa, 2002). In clinical laboratories, optochin susceptibility is a common technique used to identify *S. pneumoniae* strains, and in recent years, the optochin-resistant strains have been isolated worldwide, with this resistance being conferred by point mutations in the *atpAC* genes, as described originally (Fenoll et al., 1994). In the present study, we identified *atpAC* mutations from clinical strains that conferred optochin resistance (Cortes et al., 2008), which were then used to study the putative contribution of F_0F_1-ATPase in ATR. To compare ATR induction of *wt* and *atpAC* mutants in the same genetic background, these *atpAC* mutations were transferred into R801, a typical laboratory strain derived from strain R6 (Lefevre et al., 1979), which showed a marked decrease in ATR. Here, we demonstrated the relevance of F_0F_1-ATPase in ATR development, not only in growth media under acidic conditions, but most significantly, in macrophages, where bacterial cells must survive the acidic pH of phagosomes. It was also found that *S. pneumoniae* was able to live more than 5 h in macrophages and more than 8 h in pneumocytes (data not shown). We propose that *S. pneumoniae* needs to induce ATR to survive inside macrophages or pneumocytes for several hours, and by demonstrating that bacterial survival of the *atpC* mutants decreased in macrophages, this confirmed that F_0F_1-ATPase plays an important role not only in ATR but also in the intracellular survival of *S. pneumoniae*.

We have previously described that acidic stress was able to induce autolysis after incubation for 1 h at pH 5.9 at 37 °C (Pinas et al., 2008). Here, we considered the possibility that F_0F_1-ATPase could be also involved in the ASIL mechanism. In fact, the *atpC* mutants displayed an accelerated autolysis compared with *wt*, provoked by a modified proton pump that also altered the ATR mechanism. As both processes were induced by the same stress condition, we hypothesized that they may share some regulatory components to coordinate their functions during stress response.

It is known that the acid tolerance response in bacteria involves different mechanisms in addition to the proton pump represented by F_0F_1-ATPase. Therefore, we also investigated signal transduction systems that could control the response to acidic stress. In Gram-positive bacteria, several TCSs have been described to control ATR. *Streptococcus mutans* and *Streptococcus gordonii* are oral streptococci that are evolutively close to *S. pneumoniae* (Ferretti et al., 2004), and in both organisms, multiple two-component systems can regulate their response to acidic stress. In *S. mutans*, the CiaRH, LevSR, LiaSR, ScnKR, Hk/Rr1037/1038 and ComDE TCSs were up-regulated during adaptation to an acidic environment, but histidine kinase mutants did not induce the same level of ATR as *wt* (Gong et al., 2009). In *S. gordonii*, mutants lacking components of TCSs, such as CiaRH, ComDE and VicRK, grew more slowly in acidified media and had higher lethal pH values (Liu and Burne, 2009). In both cases, these results suggest that the multiple TCSs are required to orchestrate their respective signal transduction networks for optimal adaptation to acidic pH.

In the present work, we screened mutants of all the histidine kinase genes present in the genome of *S. pneumoniae* (Tettelin et al., 2001), and found that the CiaRH TCS was essential for ATR development, in agreement with the ATR phenotype described for other TCS mutants in streptococci. However, a contrasting phenotype was found for the *comE* mutant, which displayed an increased ATR compared with *wt*. Furthermore, ATR tests on the *comA* and *comD* mutants alone, or after the addition of synthetic CSP, indicated that ComE regulation is independent of cell density and consequently of the quorum sensing system triggered by CSP, as reported for competence state activation at pH 7.8 (Claverys et al., 2006). These results showed a clear difference to the ATR regulated by ComDE

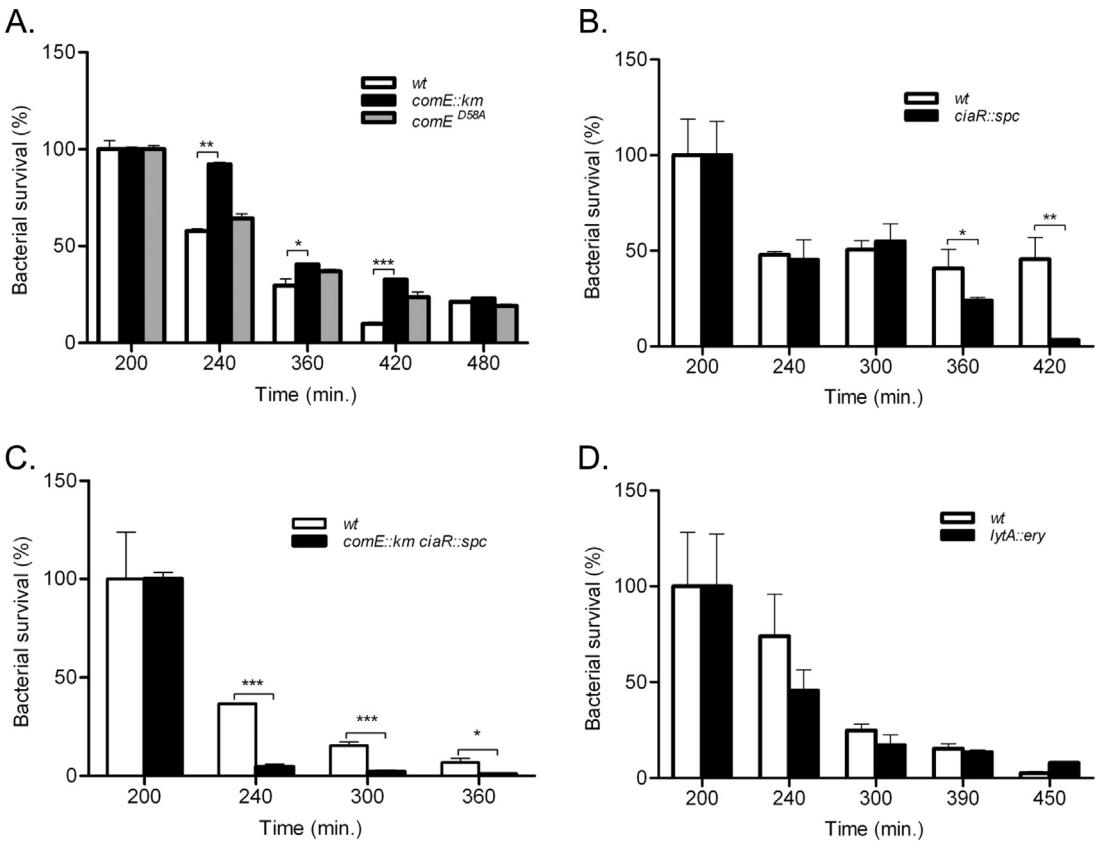

Fig. 7. ComE and CiaR control intracellular survival in A549 pneumocytes. Bacteria were initially incubated for 3 h on a monolayer of A549 cells and survival progression of *wt* vs. *comE::km* and *comE*^{D58A} (A); *ciaR::spc* (B); *comE::km ciaR::spc* (C) and *lytA::ery* (D) strains was monitored using a classical protection assay (see the Material and methods section). Survival percentages were calculated by considering the total amount of internalized bacteria after 20 min of antibiotic treatment as 100% for each strain. Statistical significance was determined by two-way ANOVA with a Bonferroni posttest, and significant differences are indicated by: * $p < 0.05$; ** $p < 0.01$; *** $p < 0.001$.

previously described in *S. gordonii* and *S. mutans*. This scenario indicates that *S. pneumoniae* uses ComE and CiaR for the response to acidic stress in order to control two opposed mechanisms that decide between survival (ATR) and suicide (ASIL).

When ASIL was blocked by mutation of the *lytA* gene, which encodes the main autolysin of *S. pneumoniae*, we expected that all acid-induced suicidal cells would be able to survive when exposed to lethal pH. However, with the *lytA* mutant, the same acid tolerance level was obtained as that of *wt*, indicating that ASIL and ATR are activated by the ComE and CiaR pathways, respectively, although this activation appear to occur in independent subpopulations.

We previously reported that ASIL was repressed in the *comE* mutant (Pinas et al., 2008), but when its ATR phenotype was analyzed, cell survival increased, suggesting that the blocked ASIL may have caused this effect. Nevertheless, as mentioned above, the *lytA* mutants did not display the same phenotype as *comE*, and as an explanation of this ATR increase of the *comE* mutants, we propose that this regulator could have had an inhibitory effect on ATR development by an unknown mechanism. Regarding to this point, the *ciaR* and *ciaH* mutants displayed normal *comE* expression under acidic conditions (Pinas et al., 2008), in contrast with the increased *comE* expression described in the *ciaR* mutant during competence development at pH 7.8 (Echenique et al., 2000), indicating that the amount of *comE* transcripts is not a factor causing of ATR repression. Therefore, the ATR inhibition found in the *ciaR* and *ciaH* mutants should be justified by the relevance that this TCS had on the ATR development. Briefly, we found that the double *ciaR comE* mutant showed a level of ATR as low as the *ciaR* mutant alone, suggesting that a dominant effect of CiaRH was present in the ComE pathway.

In reference to the probable mechanism of ASIL induction, we discarded the possibility of an increase in the *lytA* transcript level, because microarray assays showed no induction of this gene under acidic conditions (Martin-Galiano et al., 2005). The DOC-induced autolysis assays performed with both acid-induced and non-induced cells suggested that LytA expression did not experiment any concentration changes during acidic exposure, as indicated (Mellroth et al., 2012). We proposed that ASIL could be induced by translocation of LytA from intracellular to extracellular compartment, according with a model proposed by Mellroth et al., when cell growth is arrested by nutrient limitation, autolysis is activated by secretion of LytA to extracellular compartment. In our case, bacterial growth was stalled by acidic pH, as shown in Fig. S3, and autolysis appear to be activated by an extracellular LytA activity (Fig. 8A). The most relevant fact is that *comE comA* expressed an activated LytA in its surface, but this enzyme is unable to trigger autolysis by itself. This suggests that ComE could be regulating the expression of other genes that encode proteins involved in the induction of autolysis. These assays complete the proposed model, in which LytA expression on surface is regulated by CiaR and ComE under acidic conditions.

In the present study, we have demonstrated the participation of F_0F_1-ATPase in ATR and ASIL development. We have also shown that these processes are regulated by CiaRH and ComE, as well as having considered the possibility that the expression of this proton pump may be controlled at the transcriptional level by these TCSs. It was previously described that the genes encoding the subunits that constitute the F_0 (*c*, *a* and *b*) and F_1 (δ, α, γ, β and ε) complexes are expressed from the 6.6-kb *atp* operon of using a functional promoter located upstream of the *atpC* gene (Martin-Galiano

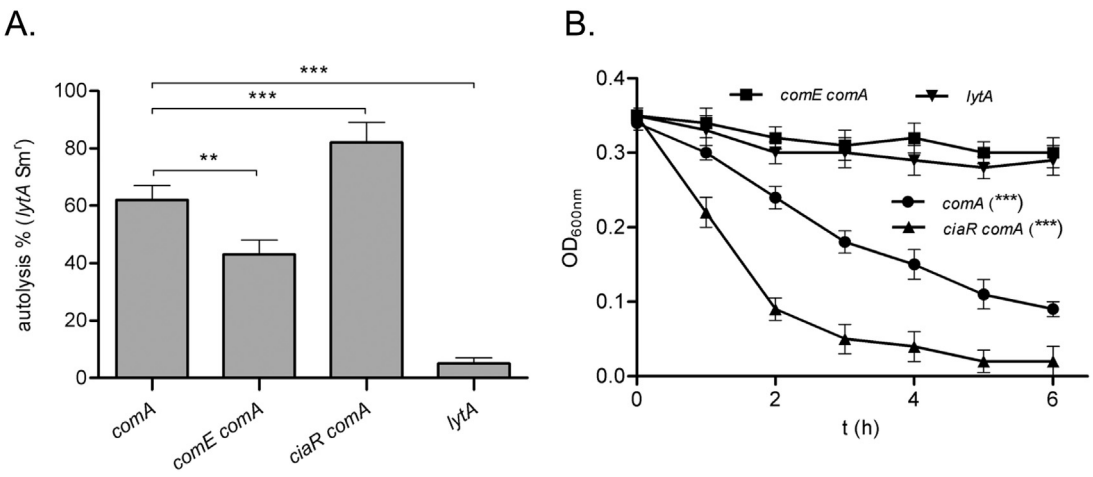

Fig. 8. ComE and CiaR control the *lytA* activity expressed on pneumococcal surface. (A) LytA activity expressed on bacterial surface was determined by a bioassay, using the Sm^R *lytA* mutant as a lysis target of the LytA activity expressed on the surface of different mutants. The *comA*, *comE comA*, *ciaR comA* and *lytA* mutants were incubated for 1 h in THYE medium at pH 5.9, and tester cells were added to the respective cultures, keeping a ratio of 3 lytA-expressing cells/1 tester cells. After 90 min of incubation, aliquots were taken and plated onto blood-TSA-agar plates containing 200 μg/ml of streptomycin. The % of lysis of the Sm^R *lytA* mutant was calculated as 100%—% of survival, considering that this strain only dies by lysis. (B) ASIL was determined in *comA* (circles), *comE comA* (squares), *ciaR comA* (up triangles), and *lytA* (down triangles) mutants cultured in THYE at pH 5.9 and at 37 °C. Cells were grown in THYE medium at pH 7.8, centrifuged and resuspended in THYE medium at pH 5.9 at 37 °C, and lysis was followed by loss of turbidity at $OD_{600\,nm}$. Data are representative of at least three independent experiments. For both panels, statistical significance was determined by one-way ANOVA with a Bonferroni posttest, and significant differences are indicated by: ** $p < 0.01$; *** $p < 0.001$.

et al., 2001). However, we could not demonstrate ComE- and CiaR-mediated regulation of the *atpC* promoter by β-galactosidase assays using a *atpC-lacZ* fusion as the reporter, although we were able to show that transcriptional activation of the *atpC* promoter increased 2.1 times when cells were exposed at pH 5.9 for 1 h, as described elsewhere (Martin-Galiano et al., 2005). In line with this result, we were unable to find the ComE-, CiaR- or ComX-binding sites (Campbell et al., 1998; Halfmann et al., 2007b; Ween et al., 1999) in the DNA region that corresponded to *atp* operon and its respective promoter region (data not shown). It has been earlier described that the *atp* gene expression was not modified in transcriptome analysis of *ciaR* and *comC* (constructed to block *comCDE* expression) mutants (Dagkessamanskaia et al., 2004). Moreover, the *rpoS* mutant showed an increased *atpC* expression in *E. coli*, suggesting that transcriptional regulation of *atp* genes is under the control of σ^S as part of a global stress response (Ito et al., 2008). In the same way, Martin-Galiano et al. suggested that the increase in *atp* mRNA shown by *S. pneumoniae* when exposed to acidic pH genes could be regulated by sigma factors induced by stress, such as σ^S in *Escherichia coli* (Espinosa-Urgel et al., 1996).

It is important to remark that the results obtained in vitro concerning signal transduction systems that control the ATR and ASIL mechanisms were also reproduced in A549 pneumocyte cultures. This suggests that ComE and CiaRH are involved in the acidic stress response of *S. pneumoniae* during its intracellular survival so that it can survive inside macrophages or pneumocytes.

When the ability to survive in pneumocytes was analyzed for the CiaR/ComE regulatory mechanism, we found that it was higher in the *comE::km* mutant than the *wt* strain in all time points, showing significant differences between them. In the last time points, the *ciaR* mutant showed a survival decrease. It was described that *S. pneumoniae* is incorporated into the eukaryotic

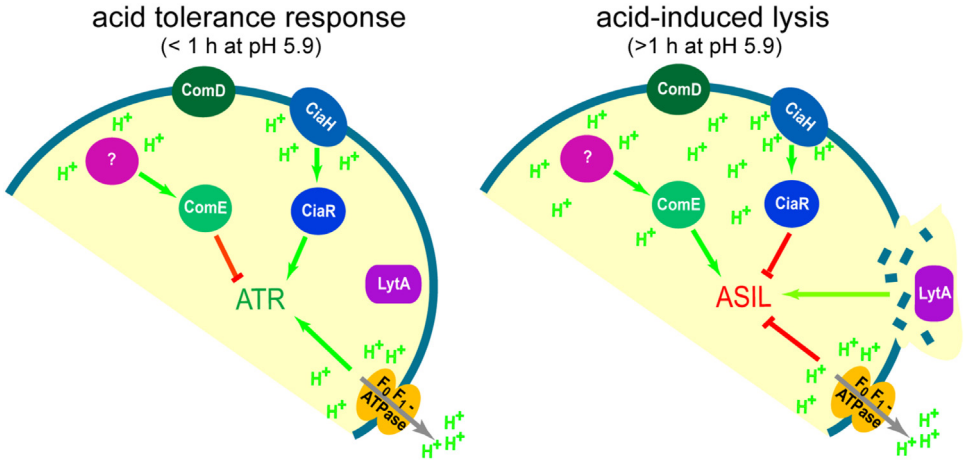

Fig. 9. Proposed model for ATR and ASIL induction of S. pneumoniae exposed to acidic conditions. Cells exposed for <1 h or >1 h at pH 5.9 induced ATR or ASIL, respectively. Green arrows indicate signaling pathways (TCS) and enzymatic reactions (F_0F_1-ATPase) that activates ATR and ASIL, in contrast, red arrows indicates when TCS or F_0F_1-ATPase block these processes. (For interpretation of the references to color in this figure legend, the reader is referred to the web version of this article.)

cells by the classical endocytic pathways, and it is a dynamic process in which bacteria underwent environmental changes, as endosomal pH (Huotari and Helenius, 2011). The survival values at different times of these mutants could respond to different pH values during the endosome maturation process, but we cannot discard other intracellular factors.

Based on our results and considerations, we propose the following model for the acidic stress response of *S. pneumoniae* (Fig. 9). When pneumococci are exposed to acidic sublethal pH, F_0F_1-ATPase contributes to ATR in an important manner by pumping protons from the bacterial cytoplasm to regulate the intracellular pH homeostasis. However, in spite of this F_0F_1-ATPase activity under acidic conditions, the intracellular pH of pneumococci should still decrease after 1–2 h of exposure. Concerning the signal transduction systems that regulate this stress response, CiaH is able to sense this environmental signal and consequently activate CiaR to develop ATR. Simultaneously, ComE is also activated by acidic stress, with the *comE* transcripts presenting a 4-fold increase after 30 min of exposure at pH 5.9 (Pinas et al., 2008), which occurs independently of its cognate histidine kinase, ComD, by means of an unknown signaling pathway. The activated ComE should trigger acid-induced autolysis after one hour of exposure at sublethal pH, and it is interestingly to note that both signaling systems affected both the ATR and ASIL processes, which represent the response to acidic stress of *S. pneumoniae*: CiaRH is essential for ATR induction while ComE has a negative control on this mechanism; in contrast, ComE is critical for ASIL induction (Pinas et al., 2008), whereas CiaRH protects against ASIL activation (Pinas et al., 2008) through an unknown mechanism. These events appear to occur in vitro as well as in the intracellular environment of the eukaryotic cells.

As mentioned above, several TCSs are involved in bacterial ATR. Concerning autolysis, many TCSs have been described to control autolysis in different bacteria, such as VraSR (Gardete et al., 2012) and ArlRS in *Staphylococcus aureus* (Memmi et al., 2012), SaeRS in *Staphylococcus epidermidis* (Lou et al., 2011), ColRS in *Pseudomonas putida* (Putrins et al., 2010), YvrGHb in *Bacillus subtillis* (Serizawa et al., 2005) LytSR and VicRK in *Streptococus gordonii* (Liu and Burne, 2011), and VicRK, ComDE (Senadheera et al., 2012) and CiaR (Gong et al., 2009) in *Streptococcus mutans*. We have highlighted the presence of ComDE and CiaRH, as these TCSs were found to be mediators of the acidic stress response in *S. pneumoniae*. Although CiaRH had the same protector function on autolysis in both *S. pneumoniae* and *S. mutans*, the ComE behavior was completely different during autolysis induction. While ComE depended on the CSP quorum-sensing system with the *comE* mutant displaying a decreased ATR in *S. mutans*, in *S. pneumoniae*, ComE regulation was independent of the quorum-sensing mechanism with the *comE* mutant showing a blocked ASIL.

Previously, we proposed that ComE is the principal route of the signaling pathway that determines a global stress response in *S. pneumoniae* (Pinas et al., 2008), and the present study strengthens this hypothesis. In addition, this is the first report of TCSs regulating a stress response that decides between a survival and a suicide mechanism. Interestingly, both ComDE (Hava and Camilli, 2002; Kowalko and Sebert, 2008; Lau et al., 2001) and CiaRH (Ibrahim et al., 2004; Sebert et al., 2002; Throup et al., 2000) have been earlier related to virulence. It is important to note the independence of the quorum sensing system in the regulation of ComE, because this regulator could only be activated by acidic pH at low cell densities in different biological niches, which has a direct implication in the control of ASIL and ATR. Summing up, this biological model contributes to the current knowledge about bacterial response under stress conditions in host tissues, where pathogens need to survive in order to establish infections, and to release virulence factors, DNA and cell wall compounds by autolysis.

Acknowledgements

We thank Don Morrison (University of Illinois at Chicago) for providing us with the chromosomal DNA from the CPM8 strain containing *comX1*/*comX2* mutations and Alex Saka for his critical review of this article. We also thank Dr L. Tao (University of Illinois at Chicago) for providing us with the pVA891 plasmid, and native speaker Dr. Paul Hobson (Cultura Británica-Argentina) for revising this manuscript. Financial support: National Council of Scientific and Technological Research (CONICET); National Agency of Scientific and Technological Promotion (ANPCYT; FONCYT PICT, Prestamo BID) and the Scientific and Technological Secretary of the National University of Cordoba (SECYT-UNC). G. Piñas had PhD fellowships from SECYT-UNC and CONICET. M. Cian had fellowships from ANPCYT, SECYT-UNC and CONICET. N. Yandar has a fellowship from ANPCYT. J. Echenique is a member of the Research Career of CONICET.

Appendix A. Supplementary data

Supplementary data associated with this article can be found, in the online version, at http://dx.doi.org/10.1016/j.ijmm.2014.12.002.

References

Albarracin Orio, A.G., Pinas, G.E., Cortes, P.R., Cian, M.B., Echenique, J., 2011. Compensatory evolution of pbp mutations restores the fitness cost imposed by beta-lactam resistance in *Streptococcus pneumoniae*. PLoS Pathog. 7, e1002000.

Andersen, N.E., Gyring, J., Hansen, A.J., Laursen, H., Siesjo, B.K., 1989. Brain acidosis in experimental pneumococcal meningitis. J. Cereb. Blood Flow Metab. 9, 381–387 (Official journal of the International Society of Cerebral Blood Flow and Metabolism).

Bassoe, C.F., Bjerknes, R., 1985. Phagocytosis by human leukocytes, phagosomal pH and degradation of seven species of bacteria measured by flow cytometry. J. Med. Microbiol. 19, 115–125.

Boudes, M., Sanchez, D., Graille, M., van Tilbeurgh, H., Durand, D., Quevillon-Cheruel, S., 2014. Structural insights into the dimerization of the response regulator ComE from *Streptococcus pneumoniae*. Nucleic Acids Res. 42, 5302–5313.

Campbell, E.A., Choi, S.Y., Masure, H.R., 1998. A competence regulon in *Streptococcus pneumoniae* revealed by genomic analysis. Mol. Microbiol. 27, 929–939.

Claverys, J.P., Dintilhac, A., Pestova, E.V., Martin, B., Morrison, D.A., 1995. Construction and evaluation of new drug-resistance cassettes for gene disruption mutagenesis in *Streptococcus pneumoniae*, using an ami test platform. Gene 164, 123–128.

Claverys, J.P., Martin, B., Polard, P., 2009. The genetic transformation machinery: composition, localization, and mechanism. FEMS Microbiol. Rev. 33, 643–656.

Claverys, J.P., Prudhomme, M., Martin, B., 2006. Induction of competence regulons as a general response to stress in gram-positive bacteria. Annu. Rev. Microbiol. 60, 451–475.

Conte, M.P., Petrone, G., Di Biase, A.M., Ammendolia, M.G., Superti, F., Seganti, L., 2000. Acid tolerance in *Listeria monocytogenes* influences invasiveness of enterocyte-like cells and macrophage-like cells. Microb. Pathog. 29, 137–144.

Cortes, P.R., Orio, A.G., Regueira, M., Pinas, G.E., Echenique, J., 2008. Characterization of in vitro-generated and clinical optochin-resistant strains of *Streptococcus pneumoniae* isolated from Argentina. J. Clin. Microb. 46, 1930–1934.

Cotter, P.D., Hill, C., 2003. Surviving the acid test: responses of gram-positive bacteria to low pH. Microbiol. Mol. Biol. Rev. 67, 429–453.

Chen, J.D., Morrison, D.A., 1987. Cloning of *Streptococcus pneumoniae* DNA fragments in *Escherichia coli* requires vectors protected by strong transcriptional terminators. Gene 55, 179–187.

Dagkessamanskaia, A., Moscoso, M., Henard, V., Guiral, S., Overweg, K., Reuter, M., Martin, B., Wells, J., Claverys, J.P., 2004. Interconnection of competence, stress and CiaR regulons in *Streptococcus pneumoniae*: competence triggers stationary phase autolysis of *ciaR* mutant cells. Mol. Microbiol. 51, 1071–1086.

Echenique, J.R., Chapuy-Regaud, S., Trombe, M.C., 2000. Competence regulation by oxygen in *Streptococcus pneumoniae*: involvement of *ciaRH* and *comCDE*. Mol. Microbiol. 36, 688–696.

Espinosa-Urgel, M., Chamizo, C., Tormo, A., 1996. A consensus structure for sigma S-dependent promoters. Mol. Microbiol. 21, 657–659.

Fenoll, A., Munoz, R., Garcia, E., de la Campa, A.G., 1994. Molecular basis of the optochin-sensitive phenotype of pneumococcus: characterization of the genes encoding the F_0 complex of the *Streptococcus pneumoniae* and *Streptococcus oralis* H(+)-ATPases. Mol. Microbiol. 12, 587–598.

Ferrandiz, M.J., de la Campa, A.G., 2002. The membrane-associated F(0)F(1) ATPase is essential for the viability of *Streptococcus pneumoniae*. FEMS Microbiol. Lett. 212, 133–138.

Ferretti, J.J., Ajdic, D., McShan, W.M., 2004. Comparative genomics of streptococcal species. Indian J. Med. Res. 119 (Suppl), 1–6.
Gardete, S., Kim, C., Hartmann, B.M., Mwangi, M., Roux, C.M., Dunman, P.M., Chambers, H.F., Tomasz, A., 2012. Genetic pathway in acquisition and loss of vancomycin resistance in a methicillin resistant *Staphylococcus aureus* (MRSA) strain of clonal type USA300. PLoS Pathog. 8, e1002505.
Giammarinaro, P., Sicard, M., Gasc, A.M., 1999. Genetic and physiological studies of the CiaH–CiaR two-component signal-transducing system involved in cefotaxime resistance and competence of *Streptococcus pneumoniae*. Microbiology 145, 1859–1869.
Gong, Y., Tian, X.L., Sutherland, T., Sisson, G., Mai, J., Ling, J., Li, Y.H., 2009. Global transcriptional analysis of acid-inducible genes in *Streptococcus mutans*: multiple two-component systems involved in acid adaptation. Microbiology 155, 3322–3332.
Gradstedt, H., Iovino, F., Bijlsma, J.J., 2013. *Streptococcus pneumoniae* invades endothelial host cells via multiple pathways and is killed in a lysosome dependent manner. PLoS One 8, e65626.
Halfmann, A., Hakenbeck, R., Bruckner, R., 2007a. A new integrative reporter plasmid for *Streptococcus pneumoniae*. FEMS Microbiol. Lett. 268, 217–224.
Halfmann, A., Kovacs, M., Hakenbeck, R., Bruckner, R., 2007b. Identification of the genes directly controlled by the response regulator CiaR in *Streptococcus pneumoniae*: five out of 15 promoters drive expression of small non-coding RNAs. Mol. Microbiol. 66, 110–126.
Hava, D.L., Camilli, A., 2002. Large-scale identification of serotype 4 *Streptococcus pneumoniae* virulence factors. Mol. Microbiol. 45, 1389–1406.
Huotari, J., Helenius, A., 2011. Endosome maturation. EMBO J. 30, 3481–3500.
Ibrahim, Y.M., Kerr, A.R., McCluskey, J., Mitchell, T.J., 2004. Control of virulence by the two-component system CiaR/H is mediated via HtrA, a major virulence factor of *Streptococcus pneumoniae*. J. Bacteriol. 186, 5258–5266.
Ito, A., May, T., Kawata, K., Okabe, S., 2008. Significance of *rpoS* during maturation of *Escherichia coli* biofilms. Biotechnol. Bioeng. 99, 1462–1471.
Konings, W.N., Otto, R., 1983. Energy transduction and solute transport in streptococci. Antonie Van Leeuwenhoek 49, 247–257.
Kowalko, J.E., Sebert, M.E., 2008. The *Streptococcus pneumoniae* competence regulatory system influences respiratory tract colonization. Infect. Immun. 76, 3131–3140.
Lau, G.W., Haataja, S., Lonetto, M., Kensit, S.E., Marra, A., Bryant, A.P., McDevitt, D., Morrison, D.A., Holden, D.W., 2001. A functional genomic analysis of type 3 *Streptococcus pneumoniae* virulence. Mol. Microbiol. 40, 555–571.
Lau, P.C., Sung, C.K., Lee, J.H., Morrison, D.A., Cvitkovitch, D.G., 2002. PCR ligation mutagenesis in transformable streptococci: application and efficiency. J. Microbiol. Methods 49, 193–205.
Lefevre, J.C., Claverys, J.P., Sicard, A.M., 1979. Donor deoxyribonucleic acid length and marker effect in pneumococcal transformation. J. Bacteriol. 138, 80–86.
Light, R.W., Girard, W.M., Jenkinson, S.G., George, R.B., 1980. Parapneumonic effusions. Am. J. Med. 69, 507–512.
Liu, Y., Burne, R.A., 2009. Multiple two-component systems of *Streptococcus mutans* regulate agmatine deiminase gene expression and stress tolerance. J. Bacteriol. 191, 7363–7366.
Liu, Y., Burne, R.A., 2011. The major autolysin of *Streptococcus gordonii* is subject to complex regulation and modulates stress tolerance, biofilm formation, and extracellular-DNA release. J. Bacteriol. 193, 2826–2837.
Lou, Q., Zhu, T., Hu, J., Ben, H., Yang, J., Yu, F., Liu, J., Wu, Y., Fischer, A., Francois, P., Schrenzel, J., Qu, D., 2011. Role of the SaeRS two-component regulatory system in *Staphylococcus epidermidis* autolysis and biofilm formation. BMC Microbiol. 11, 146.
Martin-Galiano, A.J., Ferrandiz, M.J., de la Campa, A.G., 2001. The promoter of the operon encoding the F0F1 ATPase of *Streptococcus pneumoniae* is inducible by pH. Mol. Microbiol. 41, 1327–1338.
Martin-Galiano, A.J., Overweg, K., Ferrandiz, M.J., Reuter, M., Wells, J.M., de la Campa, A.G., 2005. Transcriptional analysis of the acid tolerance response in *Streptococcus pneumoniae*. Microbiology 151, 3935–3946.
Martin, B., Granadel, C., Campo, N., Henard, V., Prudhomme, M., Claverys, J.P., 2010. Expression and maintenance of ComD–ComE, the two-component signal-transduction system that controls competence of *Streptococcus pneumoniae*. Mol. Microbiol. 75, 1513–1528.
Martin, B., Prudhomme, M., Alloing, G., Granadel, C., Claverys, J.P., 2000. Cross-regulation of competence pheromone production and export in the early control of transformation in *Streptococcus pneumoniae*. Mol. Microbiol. 38, 867–878.
Mellroth, P., Daniels, R., Eberhardt, A., Ronnlund, D., Blom, H., Widengren, J., Normark, S., Henriques-Normark, B., 2012. LytA, major autolysin of *Streptococcus pneumoniae*, requires access to nascent peptidoglycan. J. Biol. Chem. 287, 11018–11029.
Memmi, G., Nair, D.R., Cheung, A., 2012. Role of ArlRS in autolysis in methicillin-sensitive and methicillin-resistant *Staphylococcus aureus* strains. J. Bacteriol. 194, 759–767.
Molenaar, D., Bolhuis, H., Abee, T., Poolman, B., Konings, W.N., 1992. The efflux of a fluorescent probe is catalyzed by an ATP-driven extrusion system in *Lactococcus lactis*. J. Bacteriol. 174, 3118–3124.
Mortier-Barriere, I., de Saizieu, A., Claverys, J.P., Martin, B., 1998. Competence-specific induction of *recA* is required for full recombination proficiency during transformation in *Streptococcus pneumoniae*. Mol. Microbiol. 27, 159–170.
Neuhaus, K., Satorhelyi, P., Schauer, K., Scherer, S., Fuchs, T.M., 2013. Acid shock of *Listeria monocytogenes* at low environmental temperatures induces *prfA*, epithelial cell invasion, and lethality towards *Caenorhabditis elegans*. BMC Genomics 14, 285.
Park, S.Y., Kim, I.S., 2013. Identification of macrophage genes responsive to extracellular acidification. Inflamm. Res. 62, 399–406.
Peeters, B.P., de Boer, J.H., Bron, S., Venema, G., 1988. Structural plasmid instability in *Bacillus subtilis*: effect of direct and inverted repeats. Mol. Gen. Genet. 212, 450–458.
Pikis, A., Campos, J.M., Rodriguez, W.J., Keith, J.M., 2001. Optochin resistance in *Streptococcus pneumoniae*: mechanism, significance, and clinical implications. J. Infect. Dis. 184, 582–590.
Pinas, G.E., Cortes, P.R., Orio, A.G., Echenique, J., 2008. Acidic stress induces autolysis by a CSP-independent ComE pathway in *Streptococcus pneumoniae*. Microbiology 154, 1300–1308.
Putrins, M., Ilves, H., Lilje, L., Kivisaar, M., Horak, R., 2010. The impact of ColRS two-component system and TtgABC efflux pump on phenol tolerance of *Pseudomonas putida* becomes evident only in growing bacteria. BMC Microbiol. 10, 110.
Radin, J.N., Orihuela, C.J., Murti, G., Guglielmo, C., Murray, P.J., Tuomanen, E.I., 2005. beta-Arrestin 1 participates in platelet-activating factor receptor-mediated endocytosis of *Streptococcus pneumoniae*. Infect. Immun. 73, 7827–7835.
Sebert, M.E., Palmer, L.M., Rosenberg, M., Weiser, J.N., 2002. Microarray-based identification of *htrA*, a *Streptococcus pneumoniae* gene that is regulated by the CiaRH two-component system and contributes to nasopharyngeal colonization. Infect. Immun. 70, 4059–4067.
Senadheera, D.B., Cordova, M., Ayala, E.A., Chavez de Paz, L.E., Singh, K., Downey, J.S., Svensater, G., Goodman, S.D., Cvitkovitch, D.G., 2012. Regulation of bacteriocin production and cell death by the VicRK signaling system in *Streptococcus mutans*. J. Bacteriol. 194, 1307–1316.
Serizawa, M., Kodama, K., Yamamoto, H., Kobayashi, K., Ogasawara, N., Sekiguchi, J., 2005. Functional analysis of the YvrGHb two-component system of *Bacillus subtilis*: identification of the regulated genes by DNA microarray and northern blot analyses. Biosci. Biotechnol. Biochem. 69, 2155–2169.
Tettelin, H., Nelson, K.E., Paulsen, I.T., Eisen, J.A., Read, T.D., Peterson, S., Heidelberg, J., DeBoy, R.T., Haft, D.H., Dodson, R.J., Durkin, A.S., Gwinn, M., Kolonay, J.F., Nelson, W.C., Peterson, J.D., Umayam, L.A., White, O., Salzberg, S.L., Lewis, M.R., Radune, D., Holtzapple, E., Khouri, H., Wolf, A.M., Utterback, T.R., Hansen, C.L., McDonald, L.A., Feldblyum, T.V., Angiuoli, S., Dickinson, T., Hickey, E.K., Holt, I.E., Loftus, B.J., Yang, F., Smith, H.O., Venter, J.C., Dougherty, B.A., Morrison, D.A., Hollingshead, S.K., Fraser, C.M., 2001. Complete genome sequence of a virulent isolate of *Streptococcus pneumoniae*. Science 293, 498–506.
Throup, J.P., Koretke, K.K., Bryant, A.P., Ingraham, K.A., Chalker, A.F., Ge, Y., Marra, A., Wallis, N.G., Brown, J.R., Holmes, D.J., Rosenberg, M., Burnham, M.K., 2000. A genomic analysis of two-component signal transduction in *Streptococcus pneumoniae*. Mol. Microbiol. 35, 566–576.
Ween, O., Gaustad, P., Havarstein, L.S., 1999. Identification of DNA binding sites for ComE, a key regulator of natural competence in *Streptococcus pneumoniae*. Mol. Microbiol. 33, 817–827.
Werbrouck, H., Vermeulen, A., Van Coillie, E., Messens, W., Herman, L., Devlieghere, F., Uyttendaele, M., 2009. Influence of acid stress on survival, expression of virulence genes and invasion capacity into Caco-2 cells of *Listeria monocytogenes* strains of different origins. Int. J. Food Microbiol. 134, 140–146.
Wilson, K., 2001. Preparation of genomic DNA from bacteria. In: Ausubel, Frederick M., et al. (Eds.), Current Protocols in Molecular Biology. John Wiley & Sons, Inc, New Jersey (Chapter 2, Unit 2 4).
Williams, S.P., Tait-Kamradt, A.G., Norton, J.E., Albert, T.J., Dougherty, T.J., 2007. Nucleotide sequence changes between *Streptococcus pneumoniae* R6 and D39 strains determined by an oligonucleotide hybridization DNA sequencing technology. J. Microbiol. Methods 70, 65–74.